Nonlinear Optics (WiSe 2018/19)
Lecture 7: November 30, 2018
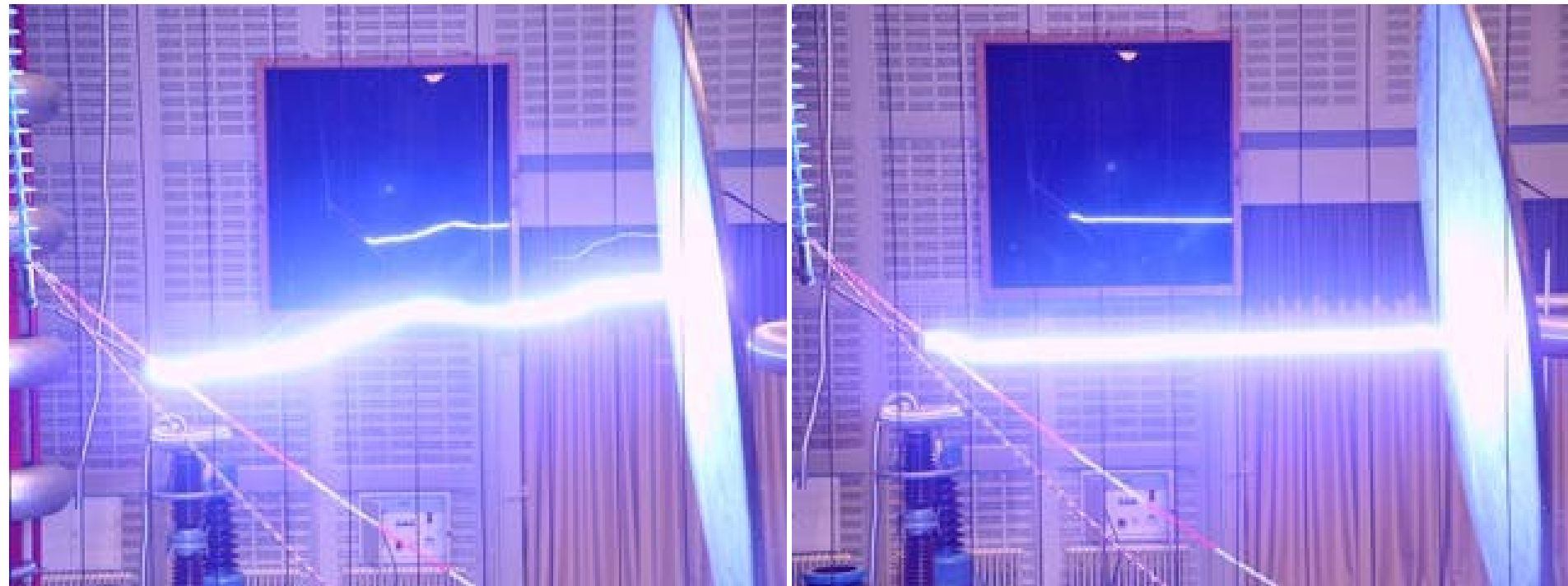
Photograph of a self-guided filament induced in air by a high-power infrared (800 nm) laser pulse   [from http://www.teramobile.org]

Remote detection of biological aerosols. The tube in the center of the picture is an open cloud chamber generating the bioaerosol simulant. The laser beam is arriving from the left. [from http://www.teramobile.org]

High-voltage lightning: (left) without laser guiding, (right) with laser guiding.
[from http://www.teramobile.org]

7.6 Raman and Brillouin scattering

Stimulated Raman and Brillouin scattering is an important technique to investigate oscillations in molecules and solids

They permit the oscillations' identification and study, without them directly coupling to the optical radiation.

stimulated Raman scattering occurring in glass fibers limits the applicable minimum pulse duration in optical communication systems

Raman amplification can be used to realize broadband Raman amplifiers for optical communications.

physical effect of Raman scattering:
light propagating though a sample with polarization fluctuations can be scattered in arbitrary direction and shifted in frequency

If the polarization fluctuations originate from oscillations of a molecules or optical or acoustic phonons in a solid, the process takes place via absorption or emission of a phonon, leading to an Anti-Stokes or Stokes shift of the photon

absorption or emission of a phonon, leading to an Anti-Stokes or Stokes shift of the photon

$$\omega_{AS} = \omega_L + \Omega \qquad (7.66)$$

$$\omega_S = \omega_L - \Omega, \qquad (7.67)$$

where ω_L is the frequency of the incident laser photon and Ω the frequency of the phonon involved in the process. A very strongly excited oscillation would contribute equally strongly to Stokes and Anti-Stokes processes. In many cases, the molecule is in the vibrational ground state, thus no thermally populated higher vibrational levels are available. In this case, the Anti-Stokes process is not possible.

SERS signal   Laser

SERS substrate
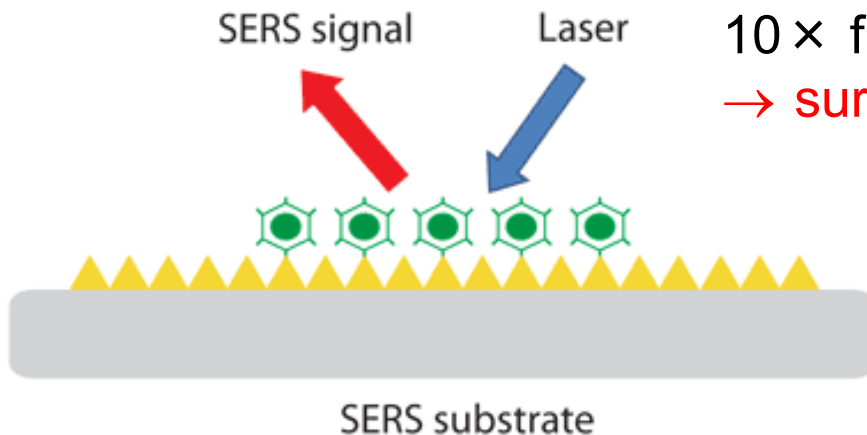
10 × field enhancement in nanostructures
→ surface-enhanced Raman scattering (SERS)
A. Campion and P. Kambhampati,
Chem. Soc. Rev. **27**, 241 (1998)

from www.semrock.com

6

For developing a model, we assume that the intramolecular oscillation co-ordinate Q of the molecule leads to a modulation of the polarizability α at optical frequencies. Then we obtain in linear response

$$\alpha = \alpha_0 + \frac{\partial \alpha}{\partial Q} \cdot Q \tag{7.68}$$

a contribution to the nonlinear polarization of the form

$$P_{NL} = N\varepsilon_0 \frac{\partial \alpha}{\partial Q} QE, \qquad \text{we need Q} \tag{7.69}$$

where we assume, that the electric field itself couples in whatever form to the intramolecular oscillation, N is the density of molecules. One form of this coupling results from the conservation of total energy, i.e., the sum of mechanical and electromagnetic energy. If the total energy is conserved, then the force exerted on the oscillation must be equal to the negative change of the stored electric energy due to the elongation of the oscillation

$$\begin{aligned}
F\delta Q &= -\delta\left\{\frac{1}{2}\varepsilon E^2\right\} = -\delta\left\{\frac{1}{2}\varepsilon_0 E^2 \left(1+\alpha\right)\right\} \tag{7.70}\\
&= -\frac{1}{2}\varepsilon_0 E^2 \delta\alpha.
\end{aligned}$$

with $\varepsilon = \varepsilon_0(1+\alpha)$. This leads to

$$F = -\frac{1}{2}\varepsilon_0 E^2 \frac{\partial \alpha}{\partial Q}. \qquad \propto E^2 \tag{7.71}$$

The oscillation amplitude then satisfies the equation

$$\frac{\partial^2 Q(t,z)}{\partial t^2} + \Gamma \frac{\partial Q(t,z)}{\partial t} + \Omega_0^2 Q(t,z) = \frac{\varepsilon_0}{2m} \frac{\partial \alpha}{\partial Q} E^2(z,t). \qquad (7.72)$$

We assume, e.g., that the electric field contains two waves at the laser frequency and the Stokes frequency, i.e.,

$$E(z,t) = E_L e^{j(\omega_L t - k_L z)} + E_S e^{j(\omega_S t - k_S z)} + c.c.$$

Since the resonance frequency of the oscillation Ω_0 is generally far below the optical frequencies ω_L and ω_S, essentially only the difference-frequency terms $\omega_L - \omega_S$ couple to the oscillation intensity modulation by beat terms

$$\frac{\partial^2 Q(t,z)}{\partial t^2} + \Gamma \frac{\partial Q(t,z)}{\partial t} + \Omega_0^2 Q(t,z) = \frac{\varepsilon_0}{2m} \frac{\partial \alpha}{\partial Q} E_L E_S^* \cdot e^{j\{(\omega_L - \omega_S)t - (k_L - k_S)z\}} + c.c.$$

$$(7.73)$$

With this we obtain for the stationary oscillation

$$Q(z,t) = \tilde{Q}(z,t) + \tilde{Q}^*(z,t) \qquad (7.74)$$

with

$$\tilde{Q}(z,t) = \frac{\frac{\varepsilon_0}{2m} \frac{\partial \alpha}{\partial Q} E_L E_S^*}{\Omega_0^2 - (\omega_L - \omega_S)^2 + j\Gamma(\omega_L - \omega_S)} e^{j\{(\omega_L - \omega_S)t - (k_L - k_S)z\}}. \qquad (7.75)$$

Within the Lorentz approximation (i.e., neglecting the off-resonant term, compare Eq. (2.29)), it follows

$$\tilde{Q}(z,t) = \frac{\frac{\varepsilon_0}{4m\Omega_0}\frac{\partial\alpha}{\partial Q}E_L E_S^*}{\Omega_0 - (\omega_L - \omega_S) + j\frac{\Gamma}{2}} e^{\,j\{(\omega_L-\omega_S)t - (k_L-k_S)z\}}. \qquad (7.76)$$

For the equation describing the Stokes wave within the SVEA, we then arrive according to Eq. (7.69) at

$$\frac{\partial E_S}{\partial z} = -\frac{j\omega_s}{cn_s}N\frac{\partial\alpha}{\partial Q}\tilde{Q}^* E_L \qquad (7.77)$$

all other beat terms ignored here

or

$$\frac{\partial E_S}{\partial z} = \frac{j\omega_S\varepsilon_0 N\left|\frac{\partial\alpha}{\partial Q}\right|^2 |E_L|^2}{4\Omega_0 mcn_s\left\{(\omega_L - \omega_S) - \Omega_0 + \frac{j\Gamma}{2}\right\}}E_S. \qquad (7.78)$$

$\chi^{(3)}$

The real part of this equation describes gain. With the intensity of the Stokes wave

$$I_S = \frac{n_s}{2}\sqrt{\frac{\varepsilon_0}{\mu_0}}|E_S|^2 \qquad (7.79)$$

follows

$$I_S(\ell) = I_{S0}\exp\{gI_L\ell\} \qquad (7.80)$$

C. V. Raman (Nobel Prize 1930)

with the Raman gain

$$g = \frac{2\omega_s N\left|\frac{\partial\alpha}{\partial Q}\right|^2}{\Omega_0 mc^2 n_s n_L\Gamma}\left\{\frac{\Gamma^2/4}{[\omega_L - \omega_S - \Omega_0]^2 + \Gamma^2/4}\right\}. \qquad (7.81)$$

Raman gain (x 10^{-13} m/W)

λ_p = 1 μm

Raman gain is superposition of several Lorentzian lines

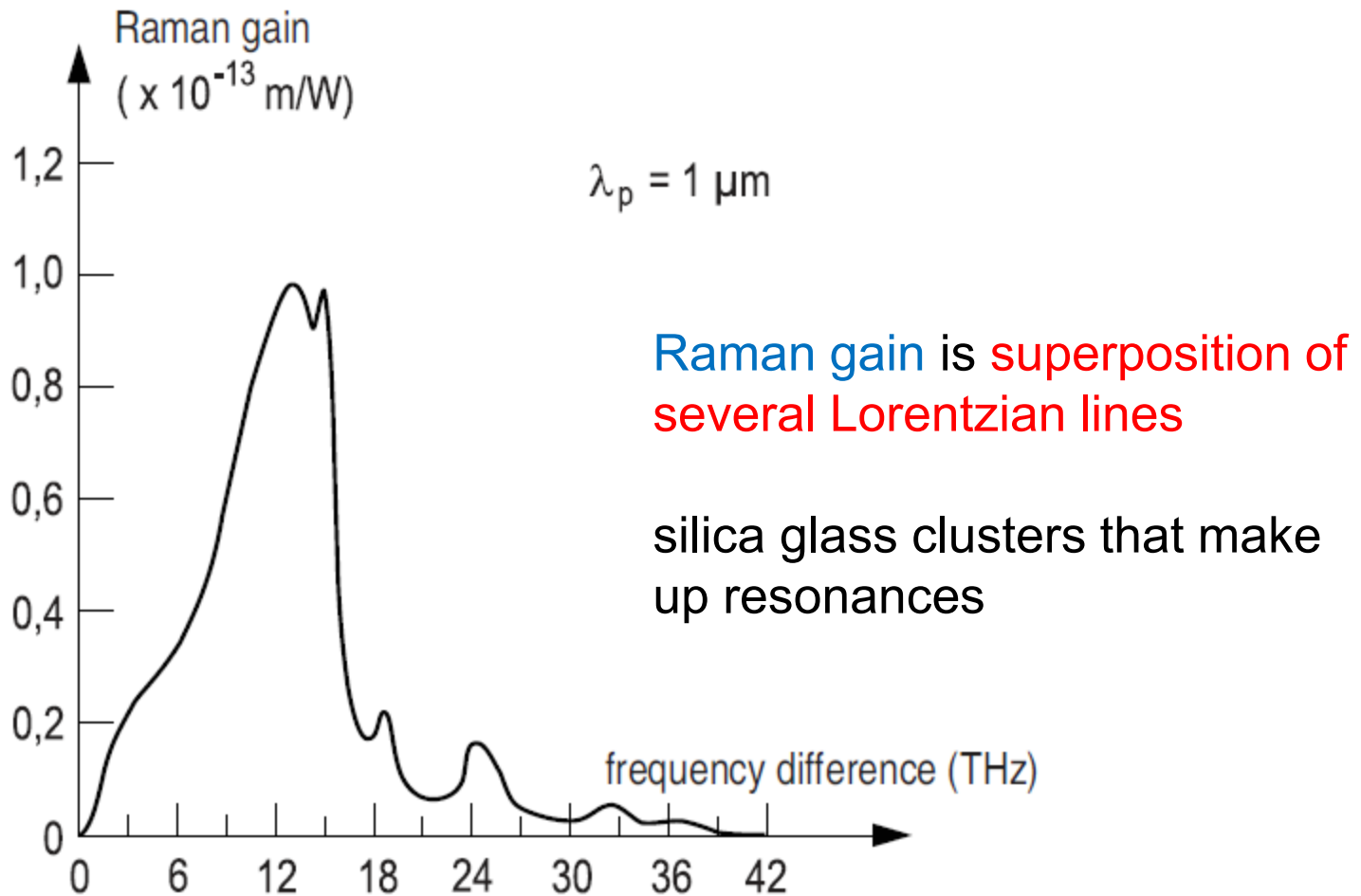silica glass clusters that make up resonances

frequency difference (THz)

Figure 7.6: Measured Raman amplification gain of melted quartz at a pump wavelength of 1 μm. The horizontal axis shows difference frequency between laser and Stokes line.

R. H. Stolen, Proc. IEEE **68**, 1232, (1980)

10

7.6.1 Focusing

For the total gain, we obtain

$$G = \int_0^{\ell} g I_L dz.$$

For a Gaussian beam, we then obtain, independent of focusing, the on-axis gain (with intensity $I_{L,\max}(z) = \dfrac{P_L}{\pi w_0^2 \left(1 + \frac{z^2}{b^2}\right)}$ and $b = \pi w_0^2 / \lambda$)

$$G_b = \int_{-\infty}^{\infty} g\, I_{L,\max} d\,z = \frac{\pi b}{\pi w_0^2} g P_L = \frac{\pi}{\lambda} g P_L.$$

We again find that the effective Raman gain, which results from a $\chi^{(3)}$-effect, in a volume is independent of focusing, as the effective interaction length is proportional to the confocal parameter b.

In contrast, we obtain for the Raman gain in a glass fiber with core radius r_0 and length ℓ

$$G_f = \frac{g P_L}{\pi r_0^2} \ell.$$

Thus the waveguiding structure enhances the Raman gain by a factor

$$\frac{G_f}{G_b} = \frac{\ell \lambda}{\pi^2 r_0^2}.$$

For a given situation, this ratio can easily amount to 10^6, e.g., for $\ell = 40$ m, $r_0 = 2$ μm and $\lambda = 1$ μm. In the real world, the effective fiber length is limited by the absorption length $1/\alpha$ for the pump light. This corresponds to several kilometers, $P_L = P_{L0} \exp\left[-\alpha z\right]$. For a long fiber ($L \gg 1/\alpha$), we obtain

$$G_f = \frac{P_{L0}}{\pi r_0^2} \left(g/\alpha\right).$$

For large gain, we can neglect the losses at the Stokes frequency. The light at the Stokes frequency emerges from initial noise, this is referred to as spontaneous scattering. A quantum treatment reveals that the power at the amplifier output originating from spontaneous processes is equivalent to 1 photon per mode at the input of the amplifier.

The output power at the Stokes frequency originating from input noise is becoming comparable to the pump power at a gain of [8]

$$G_f \cong 16,$$

and the required pump power is then given by

$$P_{L0} \cong 16 \left(A_{eff}\right) \left(\alpha/g\right).$$

For a maximum Raman gain of $g = 0.1/\text{m} \cdot \left(\mu\text{m}^2/A_{eff}\right) \cdot \left(P/\text{W}\right)$ from Fig. 7.6 and 0.2 dB damping, corresponding to an absorption length of 20 km, at the communications wavelength 1.55 μm, and $A_{eff} = 50$ μm^2, we obtain a threshold power of $P_{L0} = 600$ mW.

7.6.2 Strong conversion

For input powers far above threshold, it is possible to create several Stokes lines as shown in Fig. 7.7. If the total power of the pump pulse (P) is transferred to the first Stokes line (S_1), then in the next fiber section a conversion to (S_2) occurs, and so on.
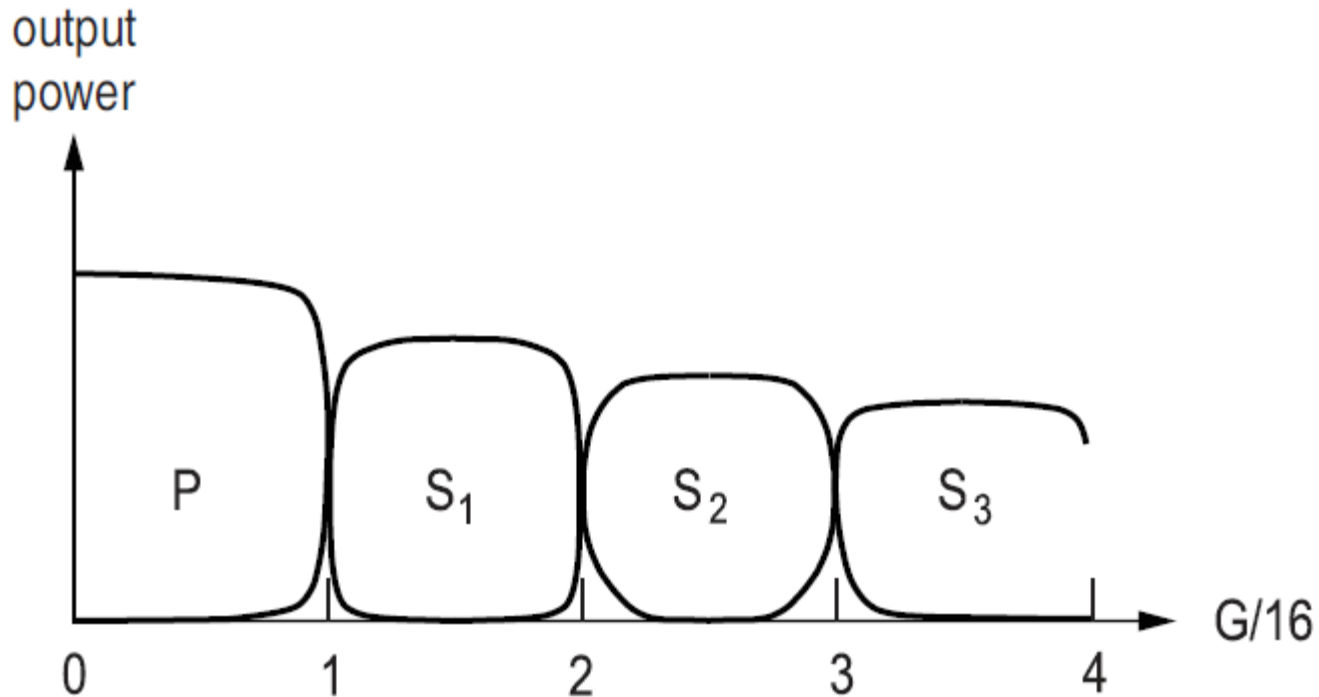
7.6.3 Stimulated Brillouin scattering

Brillouin scattering: scattering of light on acoustic waves

Again as for Raman scattering, fluctuations of polarizations, but now caused by acoustic waves, give rise to spontaneous and stimulated scattering.

First observation of Stimulated Brillouin scattering (SBS):

R. Y. Chiao, C. H. Townes, and B. P. Stoicheff, Phys. Rev. Lett. **12**, 592 (1964).

For strong pump fields: very efficient frequency conversion

In contrast

to Raman-active molecule oscillations or optical phonons, acoustic waves or phonons propagate with a velocity v_a, thus the wave number κ and frequency Ω of the acoustic wave are related by

$$\kappa = \frac{\Omega}{v_a}. \tag{7.82}$$

In the scattering process, momentum and energy must be conserved

$$\mathbf{k}_S = \mathbf{k}_L - \boldsymbol{\kappa}. \tag{7.83}$$

$$\omega_S = \omega_L - \Omega. \tag{7.84}$$

From the second condition follows

$$k_S = \frac{n_S}{n_L} k_L - \frac{n_S v_a}{c} \kappa. \tag{7.85}$$
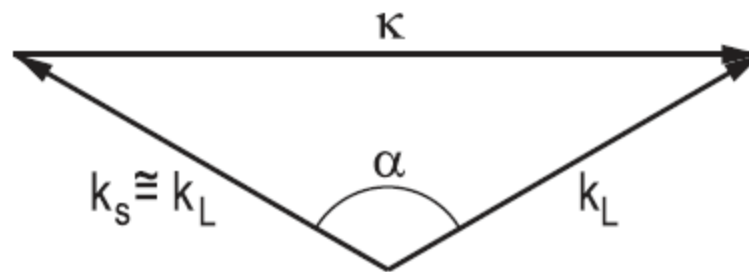
Since acoustic frequencies (kHz - 100 GHz) are much smaller than optical frequencies (300 THz), it follows $\omega_S \approx \omega_L$ and thus $k_S \approx \frac{n_S}{n_L} k_L \approx k_L$. The scattering geometry for SBS thus looks as depicted in Fig. 7.8. Furthermore, the sound velocity is much smaller than that of light, $v_a \ll c$, such that we approximately have $v_a/c \approx 10^{-5}$. The wavelength of the sound wave can thus easily become of the same order of magnitude as that of light, therefore in general arbitrary angles α are possible, i.e.,

$$\kappa \cong 2k_L \sin\frac{\alpha}{2} \quad \Rightarrow \quad \sin\frac{\alpha}{2} \cong \frac{\kappa}{2k_L} = \frac{\lambda_L}{2\Lambda n}, \tag{7.86}$$

where λ_L is the wavelength of light in the medium with refractive index n and Λ the wavelength of the sound wave. This is the same condition as the Bragg condition for scattering of X-rays from crystals. Again the longest interaction length can be achieved in a guided collinear geometry of laser and Stokes because from Eq. (7.86) and $\alpha = 0$, it follows that $\Omega_B = \kappa = 0$. However, it is possible in backscattering geometry, $\alpha = \pi$, it then holds

$$\Lambda = \frac{\lambda_L}{2n}. \tag{7.87}$$

Thus the wavelength of light in combination with the phase velocity of the sound wave and the refractive index of the material determine the frequency of the interacting sound wave via

$$\Omega_B = \frac{4\pi n v_a}{\lambda_L}. \tag{7.88}$$

For infrared light in glass with $\lambda_L = 1.55~\mu$m, $n = 1.5$, and $v_a = 5.96$ km/s, we obtain an SBS frequency of $f_B = \Omega_B/2\pi = 11.5$ GHz.

We now want to consider again the acousto-optical coupling. The amplitude of elongation is $Q(t, z) = Qe^{j(\Omega t - \kappa z)}$, which satisfies

$$\frac{\partial^2 Q(z,t)}{\partial t^2} + \Gamma\frac{\partial Q(t,z)}{\partial t} - v_a^2\frac{\partial^2 Q(t,z)}{\partial z^2} = \frac{1}{\rho}F(t,z). \qquad (7.89)$$

where ρ is the density of the medium and Γ a damping constant. The light field now couples to a wave and not to localized oscillations. In analogy to the Raman effect, the driving force is given by

$$F(t,z) = \frac{1}{2}\varepsilon_0 E^2\frac{\partial\alpha}{\partial Q}. \qquad (7.90)$$

However, we point out that here the polarizability is modulated by the stress created in the medium which is only one consequence of the oscillation elongation Q. In general, a change in the refractive index ellipsoid resulting from stress is described by the elasto-optical coefficient p

$$\Delta(1/n^2) = pS \quad\Rightarrow\quad \Delta n = -\frac{n^3}{2}pS, \qquad (7.91)$$

or

$$\Delta\alpha = \Delta(\varepsilon/\varepsilon_0) = 2n\Delta n = -n^4 pS. \qquad (7.92)$$

The stress results from the elongation Q according to

$$S = \frac{\partial Q}{\partial z} = -j\kappa Q, \tag{7.93}$$

such that

$$\frac{\partial \alpha}{\partial Q} = j\kappa n^4 p. \tag{7.94}$$

For slowly varying amplitudes (SVEA) and $\Omega^2 = v_a^2 \kappa^2$, Eq. (7.89) for the oscillation amplitude simplifies to

$$\frac{\partial Q}{\partial t} + \frac{\Gamma}{2}Q + v_a\frac{\partial Q}{\partial z} = \frac{\varepsilon_0 \kappa n_s^4 p}{4\Omega\rho} E_L E_S^*. \tag{7.95}$$

For the case of strong damping, e.g., in glass, a 50-GHz phonon only propagates only 12 μm, in the stationary state, $\partial/\partial t = \partial/\partial z = 0$, it follows

$$Q = \frac{\varepsilon_0 \kappa n_s^4 p}{2\Omega\rho\Gamma} E_L E_S^*. \tag{7.96}$$

The nonlinear polarization then is

$$P_{NL}(\omega_s) = \varepsilon_0 \frac{\partial \alpha}{\partial Q} Q^* \cdot E_L = j\kappa\varepsilon_0 n_s^4 p Q^* E_L. \tag{7.97}$$

The backwards scattered Brillouin radiation then grows exponentially according to

$$\frac{\partial E_S}{\partial z} = \frac{j\omega_s}{2cn_s\varepsilon_0}P_{NL} = -\frac{\kappa^2 n_s^7 p^2 \omega_s \varepsilon_0}{4c_0 \Omega \rho \Gamma}\left|E_L\right|^2 E_S$$

or

$$\frac{\partial I_S}{\partial z} = -gI_L I_S$$

with

$$g = \frac{8\pi^2 n_s^6 p^2}{\lambda_s^2 c_0 \rho v_a \Gamma} = \frac{4\pi n_s^6 p^2}{\lambda_s^2 c_0 \rho v_a \Delta\nu_B},$$

where $\Delta\nu_B = \Gamma/2\pi$ is the FWHM bandwidth for Brillouin scattering. Due to the narrower bandwidth $\Delta\nu_B$ on the order of a few to 100 MHz, Brillouin amplification is typically much stronger than Raman amplification. However, only pump light within a bandwidth $\Delta\nu_B$ contributes to Brillouin amplification at a certain frequency. Therefore, by using pulses with durations below 1 ns, whose spectrum is narrower than 300 MHz, one can suppress Brillouin scattering. For the propagation of ps (or even shorter) pulses, Brillouin scattering plays often no role. In contrast, when using narrowband lasers with linewidths below 10 MHz, the threshold for strong Brillouin scattering is reduced to a few mW. The threshold for Brillouin backscattering is ~ 20.

The backwards scattered Brillouin radiation then grows exponentially according to

$$\frac{\partial E_S}{\partial z} = \frac{j\omega_s}{2cn_s\varepsilon_0} P_{NL} = -\frac{\kappa^2 n_s^7 p^2 \omega_s \varepsilon_0}{4c_0 \Omega \rho \Gamma} |E_L|^2 E_S$$

or

$$\frac{\partial I_S}{\partial z} = -gI_L I_S$$

with

$$g = \frac{8\pi^2 n_s^6 p^2}{\lambda_s^2 c_0 \rho v_a \Gamma} = \frac{4\pi n_s^6 p^2}{\lambda_s^2 c_0 \rho v_a \Delta \nu_B},$$

where $\Delta \nu_B = \Gamma/2\pi$ is the FWHM bandwidth for Brillouin scattering. Due to the narrower bandwidth $\Delta \nu_B$ on the order of a few to 100 MHz, Brillouin amplification is typically much stronger than Raman amplification. However, only pump light within a bandwidth $\Delta \nu_B$ contributes to Brillouin amplification at a certain frequency. Therefore, by using pulses with durations below 1 ns, whose spectrum is narrower than 300 MHz, one can suppress Brillouin scattering. For the propagation of ps (or even shorter) pulses, Brillouin scattering plays often no role. In contrast, when using narrowband lasers with linewidths below 10 MHz, the threshold for strong Brillouin scattering is reduced to a few mW. The threshold for Brillouin backscattering is ~ 20.

8 Optical Solitons

$$\begin{aligned}
\mathbf{E}(z,t) &= E(z,t)\mathbf{e}_x \\
E(z,t) &= Re\left\{\hat{E}(\omega)e^{j(\omega t - kz)}\right\} \\
&= |\hat{E}|\cos(\omega t - kz + \varphi),
\end{aligned} \tag{8.1}$$

where $k(\omega) = \omega n(\omega)/c_0$, with n the refractive index of the medium. In general the refractive index depends on frequency, and we want to understand the propagation of a pulse with carrier frequency ω_0 (see Fig. 8.1)

$$E(z,t) = Re\left\{\frac{1}{2\pi}\int_0^\infty \hat{E}(\omega)e^{i(\omega t - k(\omega)z)}d\omega\right\}. \tag{8.2}$$
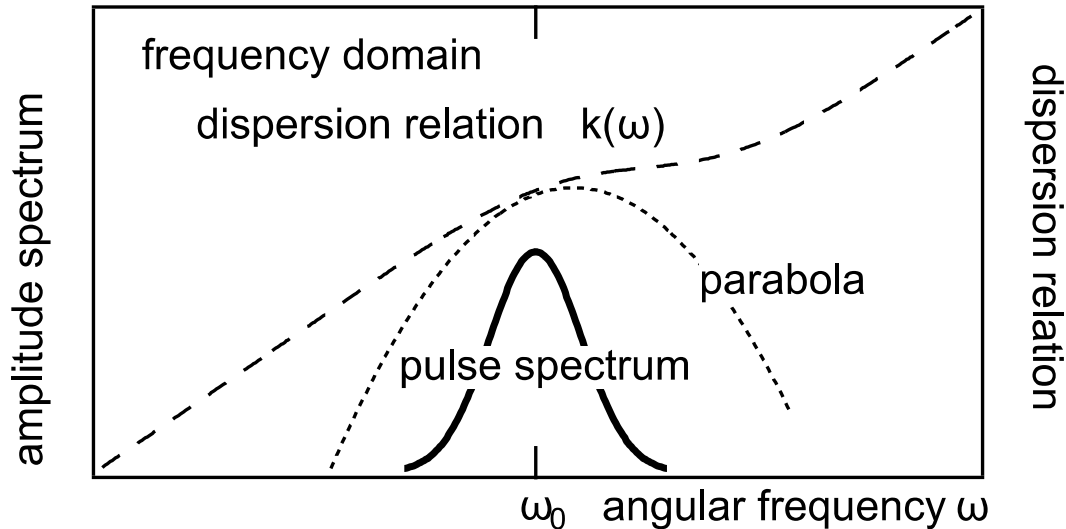
Figure 8.1: Spectral density and dispersion relation for an optical pulse.
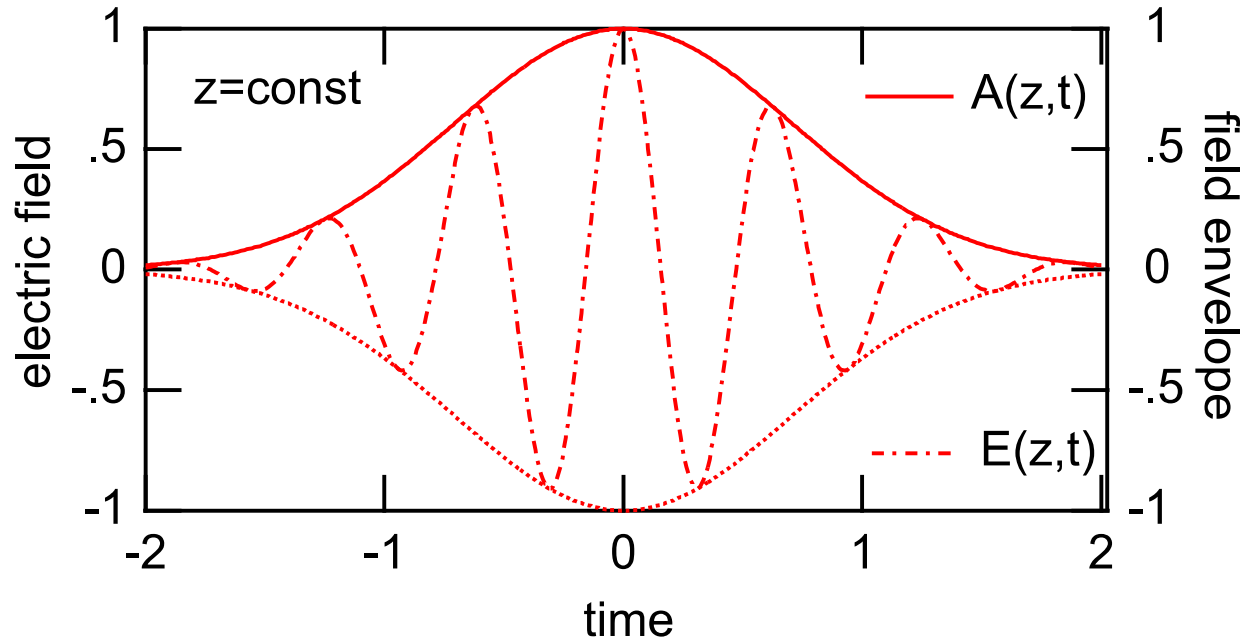
Figure 8.2: Decomposition of a pulse into carrier wave and envelope.

The electric field of the pulse in Eq. (8.2) can be decomposed into a carrier wave and an envelope $A(z,t)$ and we normalize the wave such that its magnitude square is the average intensity

$$E(z,t) = \sqrt{\frac{2Z_0}{n(\omega_0)}} Re\left\{ A(z,t)e^{j(\omega_0 t - k(\omega_0)z)} \right\}. \qquad (8.3)$$

The envelope is then defined as

$$A(z,t) = \frac{1}{2\pi} \int_{-\omega_0 \to -\infty}^{\infty} \hat{A}(\Delta\omega) e^{j(\Delta\omega t - \Delta k(\Delta\omega)z)} d\Delta\omega, \qquad (8.4)$$

where

$$\Delta\omega = \omega - \omega_0, \qquad (8.5)$$

$$\Delta k(\Delta\omega) = k(\omega_0 + \Delta\omega) - k(\omega_0), \qquad (8.6)$$

$$\tilde{A}(\Delta\omega) = \tilde{E}(\omega = \omega_0 + \Delta\omega)\sqrt{\frac{2Z_0}{n(\omega_0)}}, \qquad (8.7)$$

as shown in Fig. 8.2.

8.1 Dispersion

$$k(\omega) = k(\omega_0) + k'|_{\omega_0}\Delta\omega + \frac{k''|_{\omega_0}}{2}\Delta\omega^2 + \frac{k'''|_{\omega_0}}{6}\Delta\omega^3 + O(\Delta\omega^4). \qquad (8.8)$$
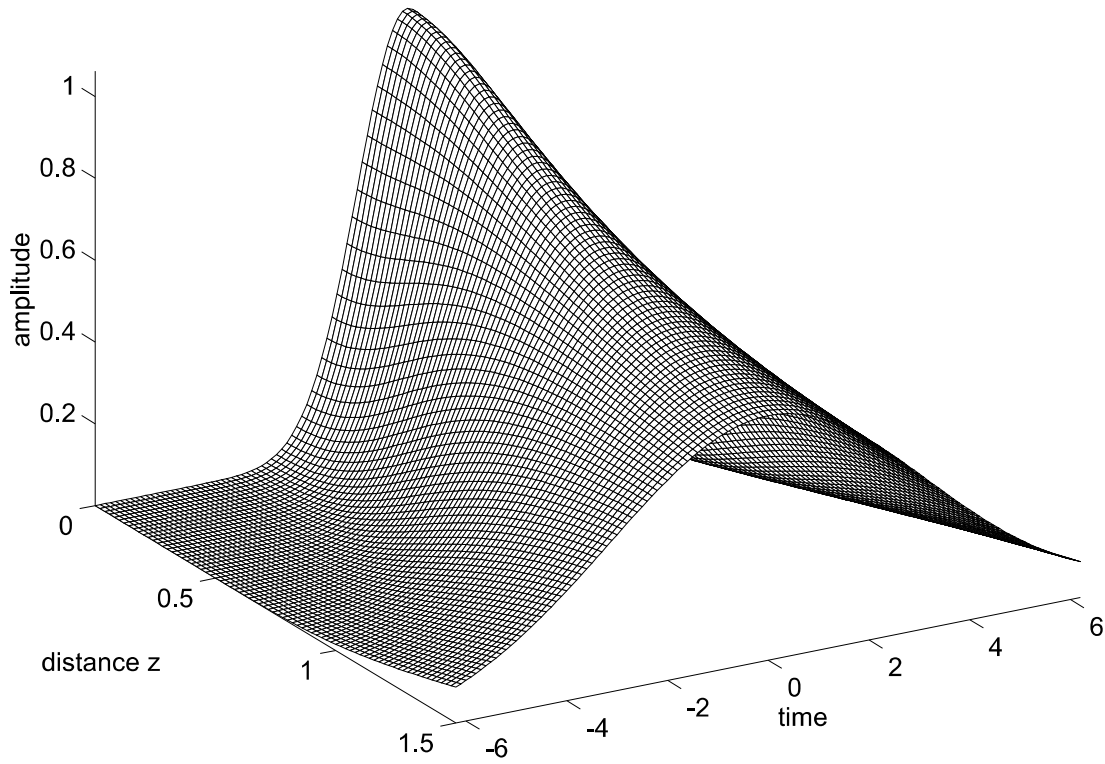
Figure 8.3: Amplitude $|A(z,t)|$ of a Gaussian pulse during propagation due to dispersion.

$$A(z, t) = A(0, t - z/v_g), \tag{8.9}$$

where $v_g = 1/k'$. Again, we introduce the retarded time, $t' = t - z/v_g$, such that

$$A(z, t') = A(0, t'). \tag{8.10}$$

When the spectrum becomes more broadband, then the second term in Eq. (8.8) becomes important, which is the group-velocity dispersion (GVD), i.e., wave packets with different carrier frequency propagate with different speeds (8.4). The envelope obeys the equation

$$\frac{\partial A(z, t')}{\partial z} = j \frac{k''}{2} \frac{\partial^2 A(z, t')}{\partial t'^2}. \tag{8.11}$$

$$\frac{\partial A(z, t')}{\partial z} = -j \sum_{n=2}^{\infty} \frac{k^{(n)}}{n!} \left(-j \frac{\partial}{\partial t'} \right)^n A(z, t'). \tag{8.12}$$

8.2 Self-phase modulation

$$n = n(\omega, |A|^2) \approx n_0(\omega) + n_2^I |A|^2. \tag{8.13}$$

The envelope of the optical pulse then follows

$$\frac{\partial A(z,t)}{\partial z} = -jk_0 n_2 |A(z,t)|^2 A(z,t) = -j\delta |A(z,t)|^2 A(z,t), \tag{8.14}$$

Self-phase modulation
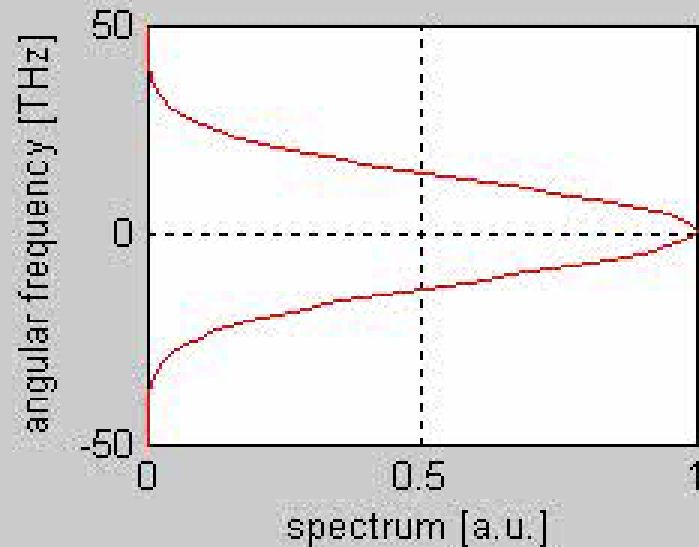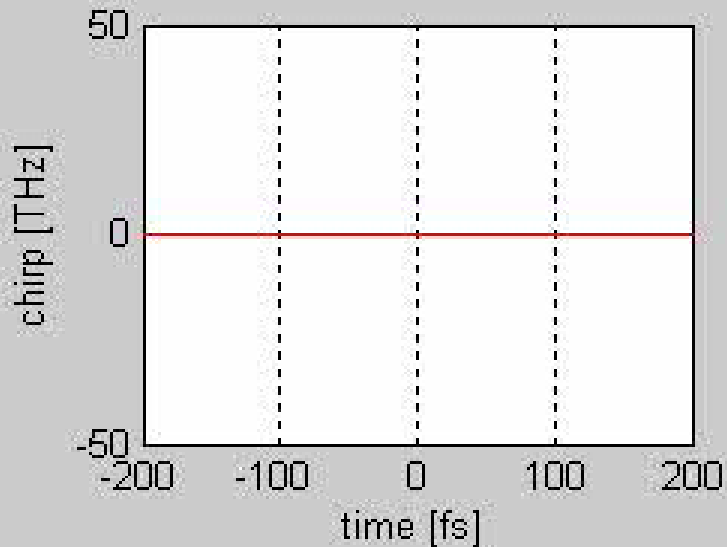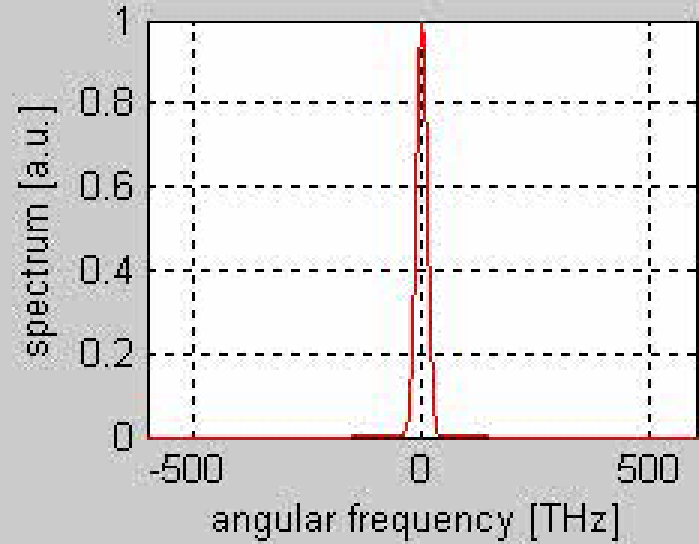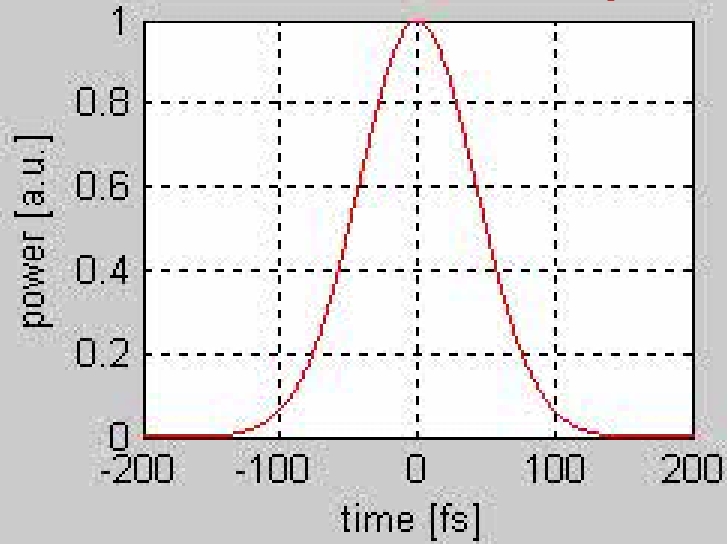
Input: Gaussian pulse, Pulse duration = 100 fs, Peak power = 1 kW

8.3 Nonlinear Schrödinger Equation (NLSE)

$$-j\frac{\partial A(z,t)}{\partial z} = \frac{k''}{2}\frac{\partial^2 A}{\partial t^2} - \delta|A|^2 A. \qquad (8.15)$$

John Scott Russell

(1808-1882)
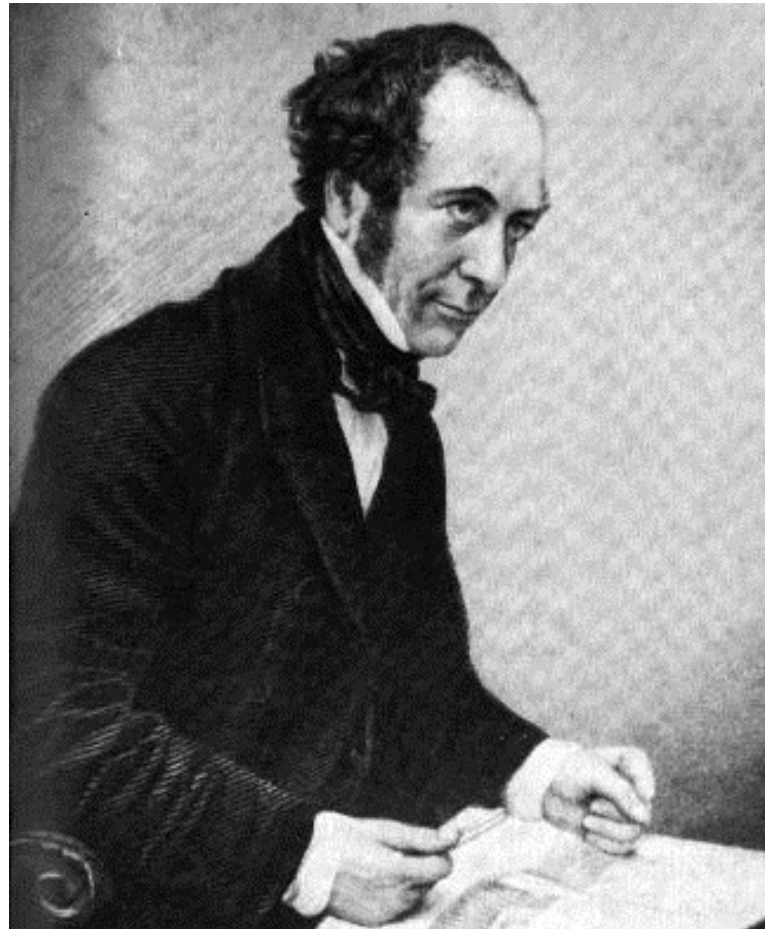
8.3 Nonlinear Schrödinger Equation (NLSE)
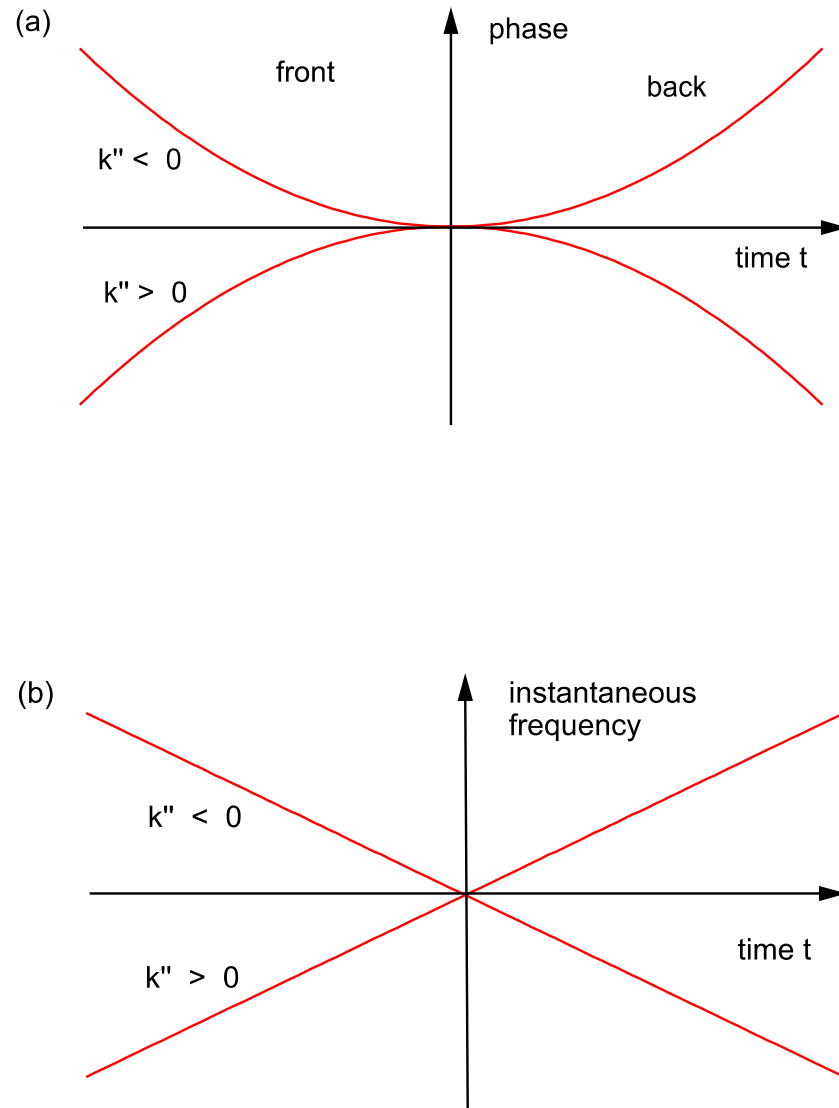
Figure 8.4: (a) Phase, (b) instantaneous frequency in a Gaussian pulse propagating in a positive dispersive medium.

29

John Scott Russel

In 1834, while conducting experiments to determine the most efficient design for canal boats, John Scott Russell made a remarkable scientific discovery. As he described it in his "Report on Waves":

Report of the fourteenth meeting of the British Association for the Advancement of Science, York, September 1844 (London 1845), pp 311-390, Plates XLVII-LVII).

Russell's report

"I was observing the motion of a boat which was rapidly drawn along a narrow channel by a pair of horses, when the boat suddenly stopped - not so the mass of water in the channel which it had put in motion; it accumulated round the prow of the vessel in a state of violent agitation, then suddenly leaving it behind, rolled forward with great velocity, assuming the form of a large solitary elevation, a rounded, smooth and well-defined heap of water, which continued its course along the channel apparently without change of form or diminution of speed."

Russell's report

"I followed it on horseback, and overtook it still rolling on at a rate of some eight or nine miles an hour, preserving its original figure some thirty feet long and a foot to a foot and a half in height. Its height gradually diminished, and after a chase of one or two miles I lost it in the windings of the channel. Such, in the month of August 1834, was my first chance interview with that singular and beautiful phenomenon which I have called the Wave of Translation."

Scott Russell Aqueduct

89.3m long, 4.13m wide,1.52m deep, On the union Canal, Near Heroit-Watt Univ.

*www.spsu.edu/math/txu/research/presentations/**soliton/talk**.ppt*

Scott Russell Aqueduct

Solitary wave

*www.spsu.edu/math/txu/research/presentations/**soliton/talk**.ppt*

A brief history (mainly for optical soliton)

- 1838 – observation of soliton in water

- 1895 – mathematical description of waves on shallow water surfaces, i.e. KdV equation

- 1972 – optical solitons arising from NLSE

- 1980 – experimental demonstration

- 1990's – soliton control techniques

- 2000's –understanding soliton in the context of supercontinuum generation

8.4 The Solitons of the NLSE

Without loss of generality, by normalization of the field amplitude $A = \frac{A'}{\tau}\sqrt{\frac{2D_2}{\delta}}$, the propagation distance $z = z' \cdot \tau^2/D_2$, and the time $t = t' \cdot \tau$, the NLSE (8.15) reads

$$j\frac{\partial A(z,t)}{\partial z} = \frac{\partial^2 A}{\partial t^2} + 2|A|^2 A. \qquad (8.16)$$

8.4.1 The fundamental soliton

$$A_s(z,t) = A_0 \text{sech}\left(\frac{t}{\tau}\right) e^{-j\theta}, \qquad (8.17)$$

where θ is the nonlinear phase shift of the soliton

$$\theta = \frac{1}{2}\delta A_0^2 z. \qquad (8.18)$$

$$\theta = \frac{|k''|}{2\tau^2}z. \tag{8.19}$$

Since the field amplitude $A(z,t)$ is normalized, such that the absolute square is the intensity, the soliton energy fluence is given by

$$w = \int_{-\infty}^{\infty} |A_s(z,t)|^2 dt = 2A_0^2\tau. \tag{8.20}$$
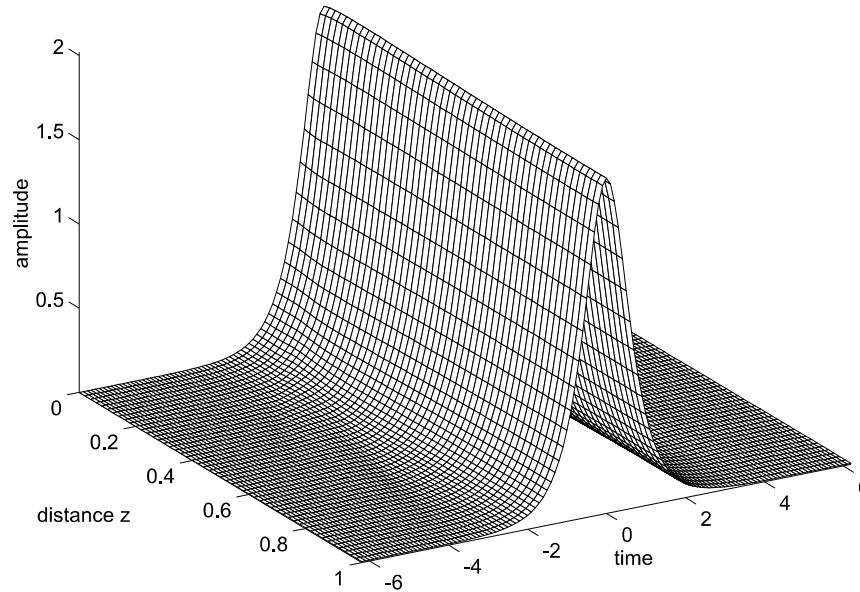
Figure 8.6: Fundamental soliton of the NLSE.

Propagation of fundamental soliton
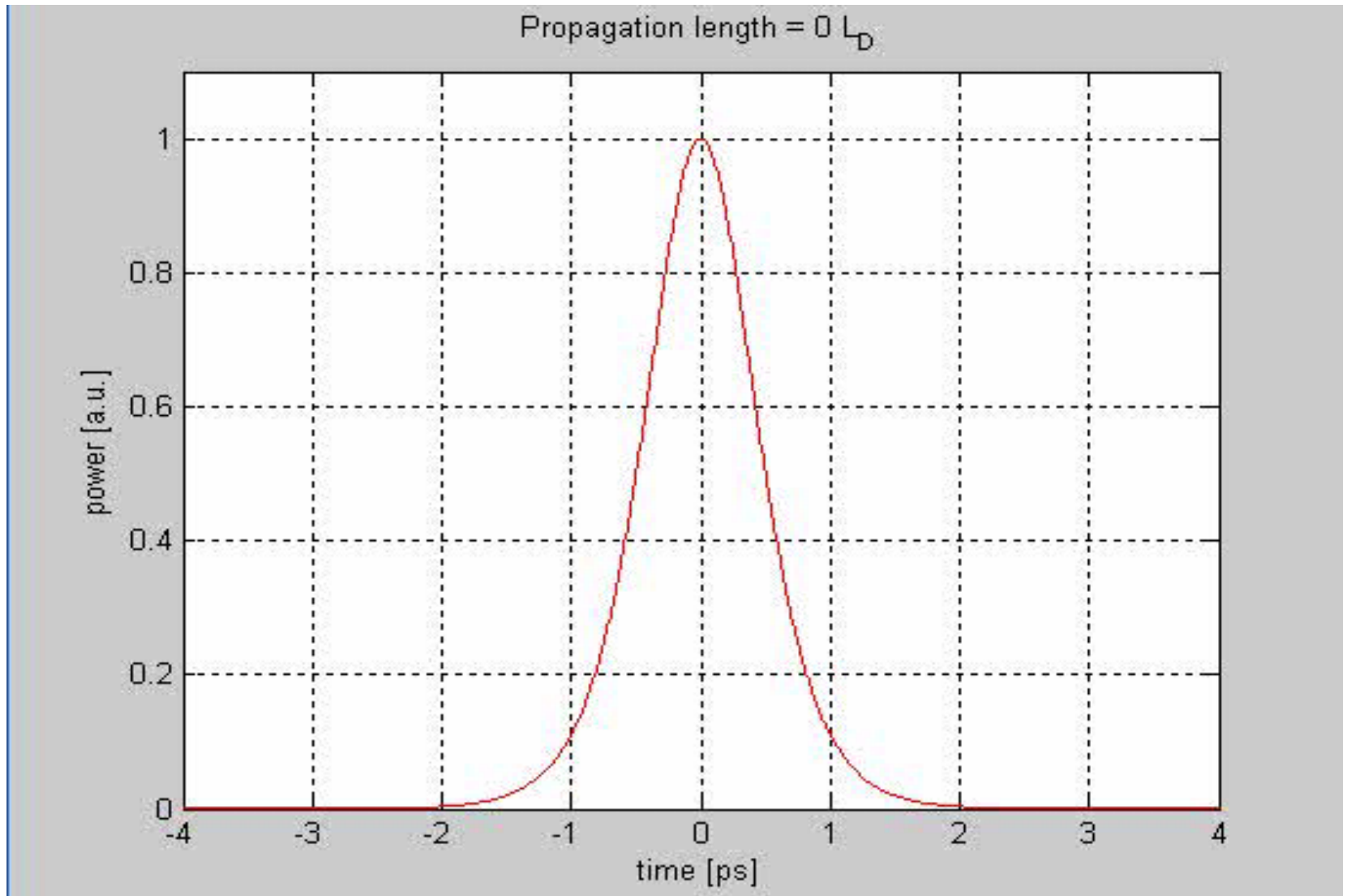
Input: 1ps soliton centered at 1.55 um; medium: single-mode fiber

Important Relations

$$\delta A_0^2 = \frac{2|D_2|}{\tau^2} \left(= \frac{|\beta_2|}{\tau^2}\right) \quad \Longrightarrow \quad A_s(z,t) = A_0 \mathrm{sech}\left(\frac{t}{\tau}\right) e^{-j\theta}$$

(Balance between dispersion and nonlinearity)

Nonlinear phase shift soliton acquires during propagation:

$$\theta = \frac{1}{2}\delta A_0^2 z = \frac{|D_2|}{\tau^2} z$$

Area Theorem

$$\mathrm{Pulse\ Area} = \int_{-\infty}^{\infty} |A_s(z,t)| dt = \pi A_0 \tau = \pi \sqrt{\frac{2|D_2|}{\delta}}.$$

Soliton Energy: $\quad w = \int_{-\infty}^{\infty} |A_s(z,t)|^2 dt = 2A_0^2 \tau \quad$ **Pulse width:** $\quad \tau = \frac{4|D_2|}{\delta w}$

39

General fundamental soliton

$$A_s(z,t) = A_0\text{sech}(x(z,t))e^{-j\theta(z,t)}, \qquad (8.23)$$

with

$$x = \frac{1}{\tau}(t - |k''|p_0 z - t_0), \qquad (8.24)$$

and the generalized phase shift

$$\theta = p_0(t - t_0) + \frac{|k''|}{2}\left(\frac{1}{\tau^2} - p_0^2\right)z + \theta_0. \qquad (8.25)$$

Higher-order Solitons: periodical evolution in both the time and the frequency domain

$$A_0\tau = N\sqrt{\frac{2|D_2|}{\delta}}, N = 1,2,3... \qquad u(0,\tau) = N\,\text{sech}(\tau)$$

G. P. Agrawal, *Nonlinear fiber optics* (2001)
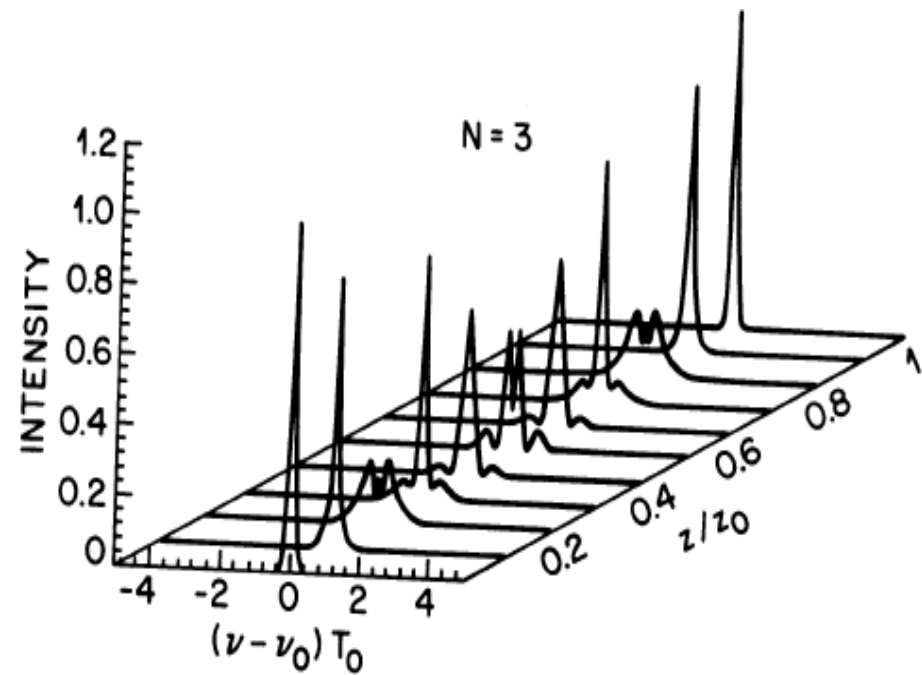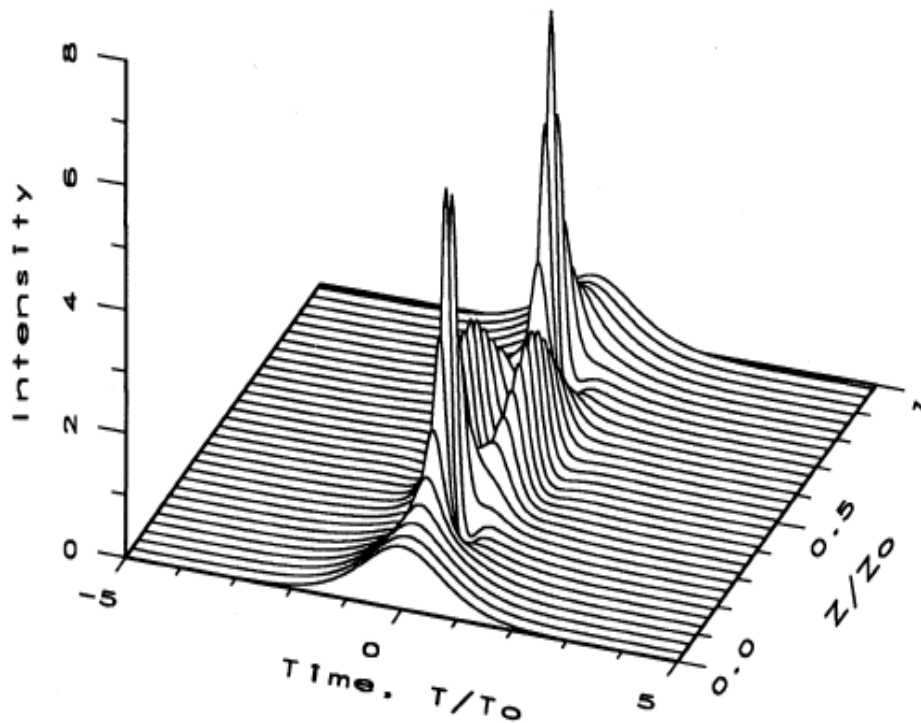
Interaction between solitons (soliton collision)
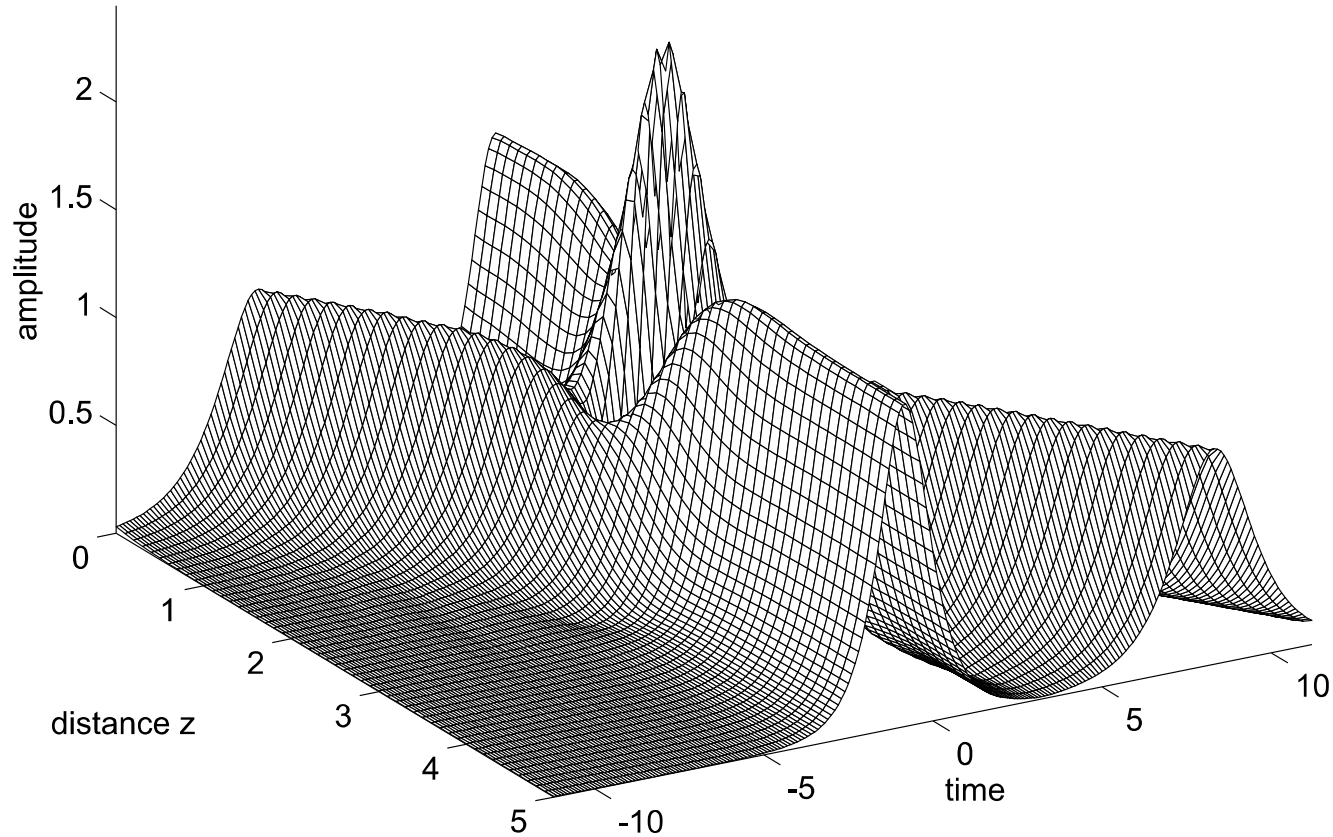
Figure 8.7: Soliton collision, both pulses recover completely.

Interaction of two solitons at the same center frequency

Input to NLSE: $u(0, \tau) = \text{sech}(\tau - q_0) + r\,\text{sech}[r(\tau + q_0)]e^{i\theta}$
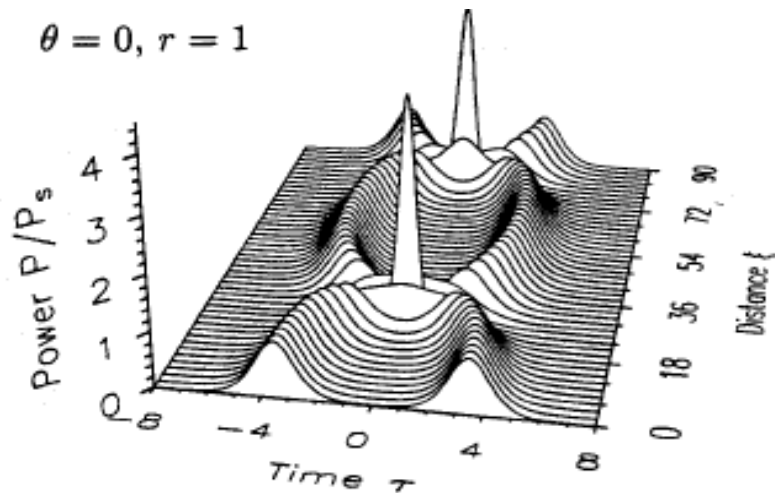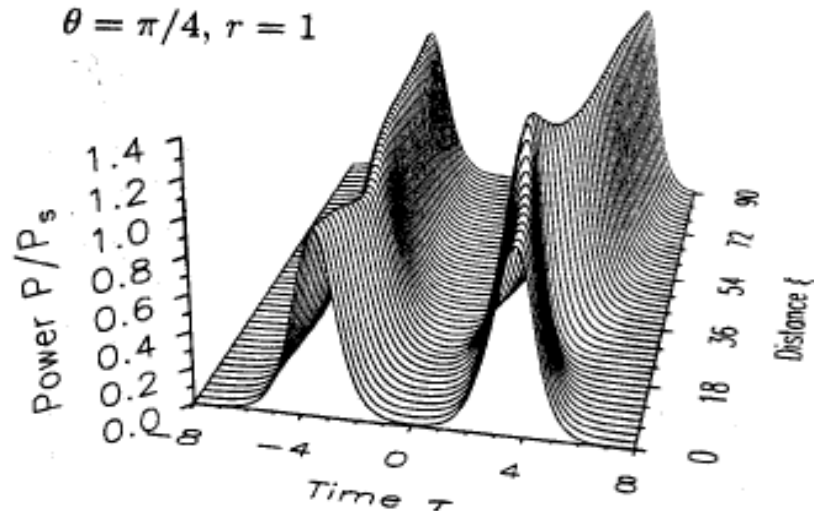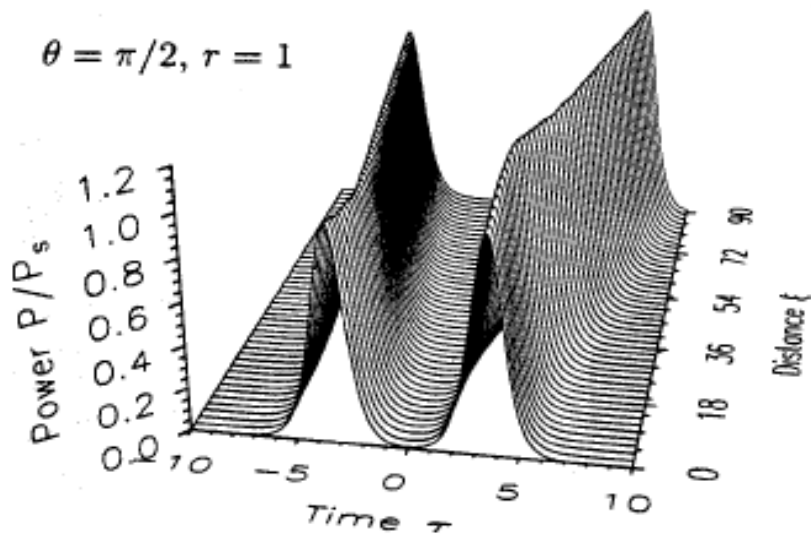
G. P. Agrawal, *Nonlinear fiber optics* (2001)
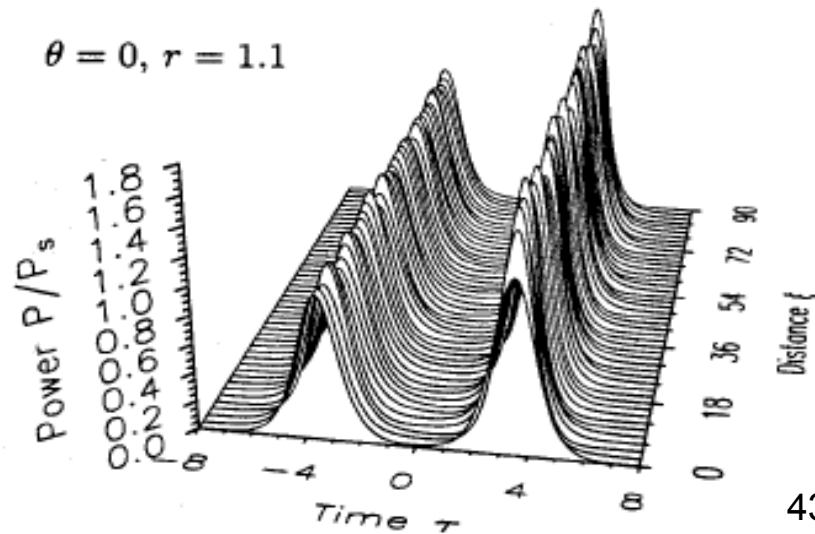
Interactions of two solitons
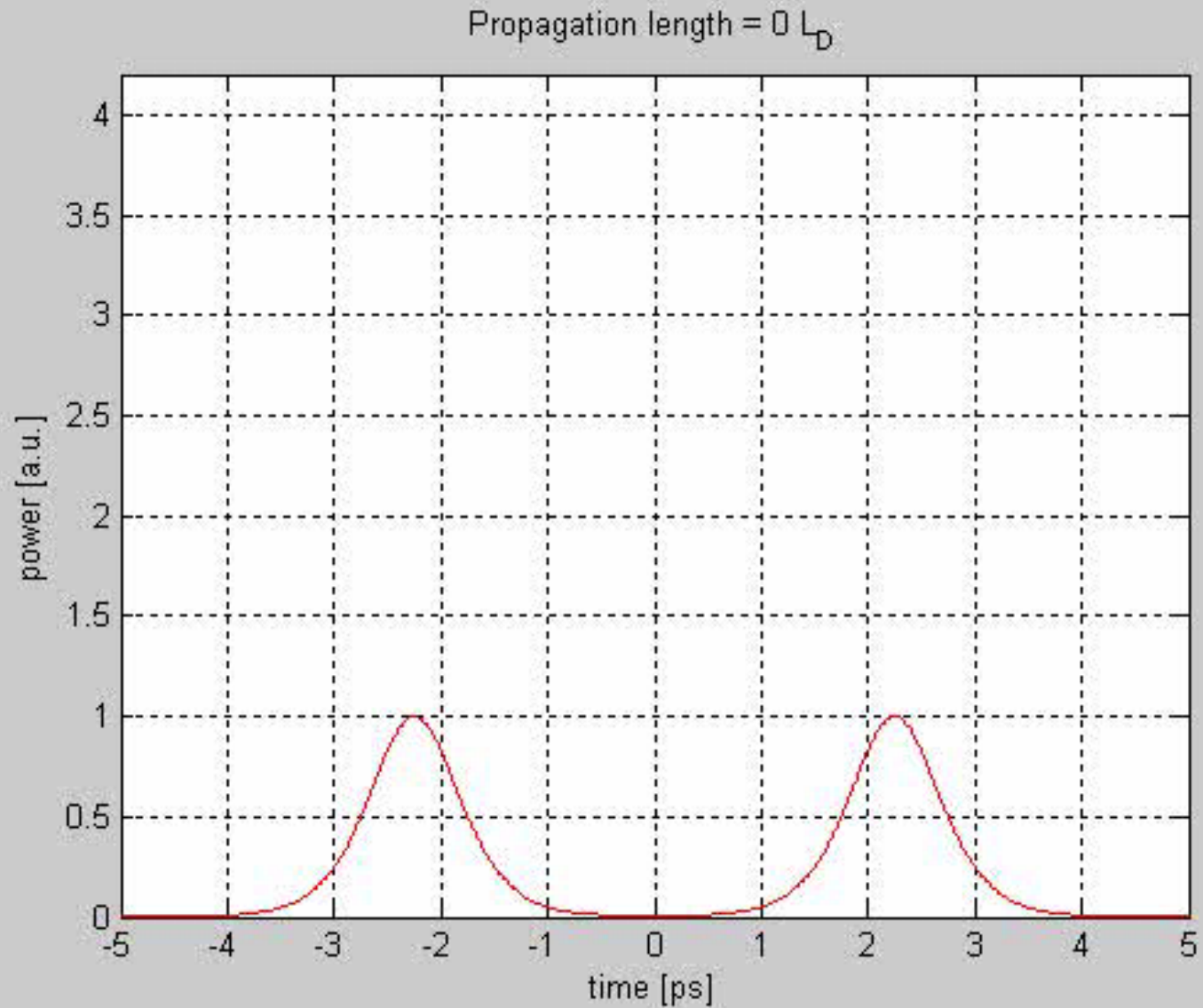
From Gaussian pulse to soliton
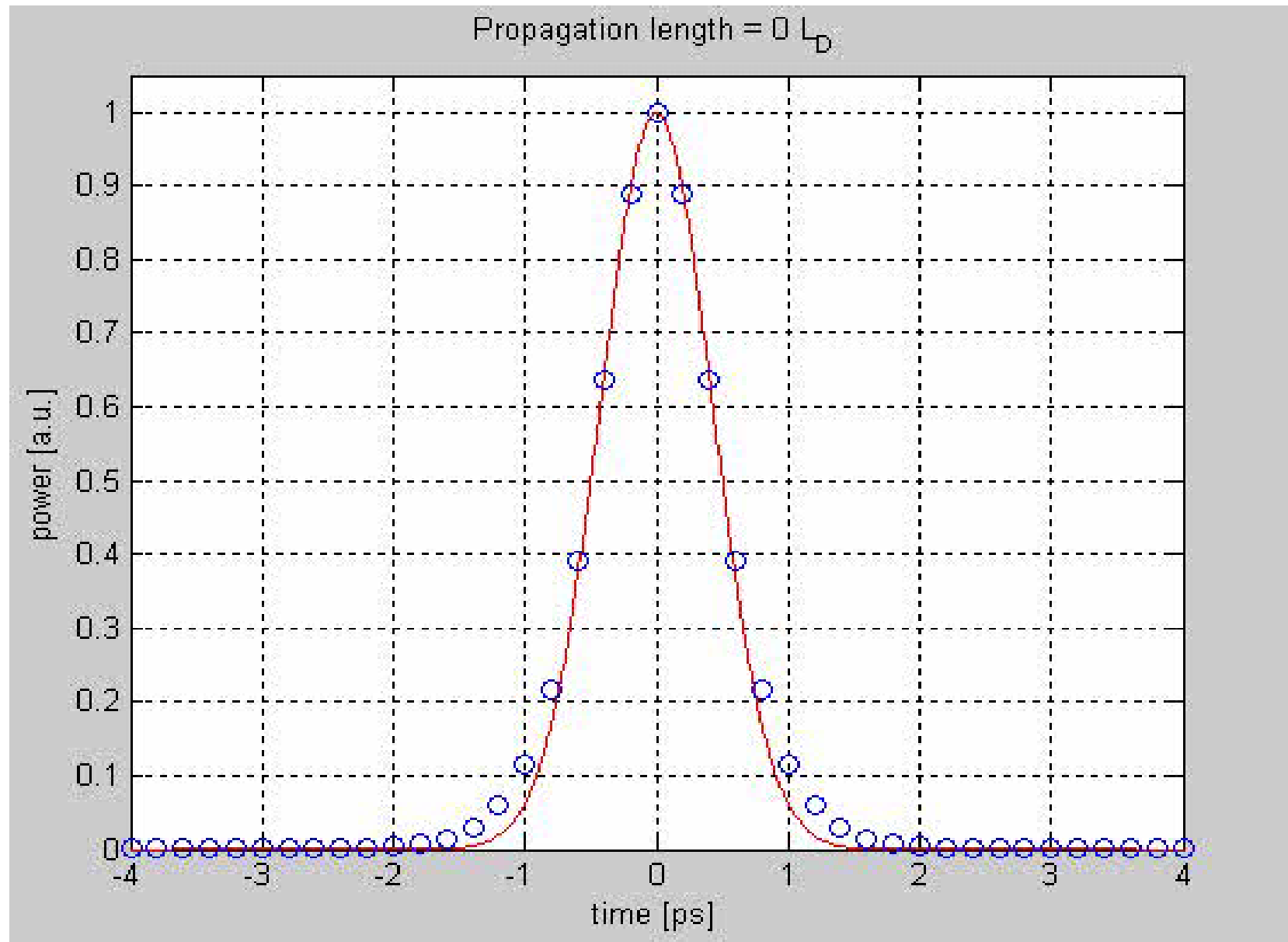
Gaussian pulse to 3-order soliton
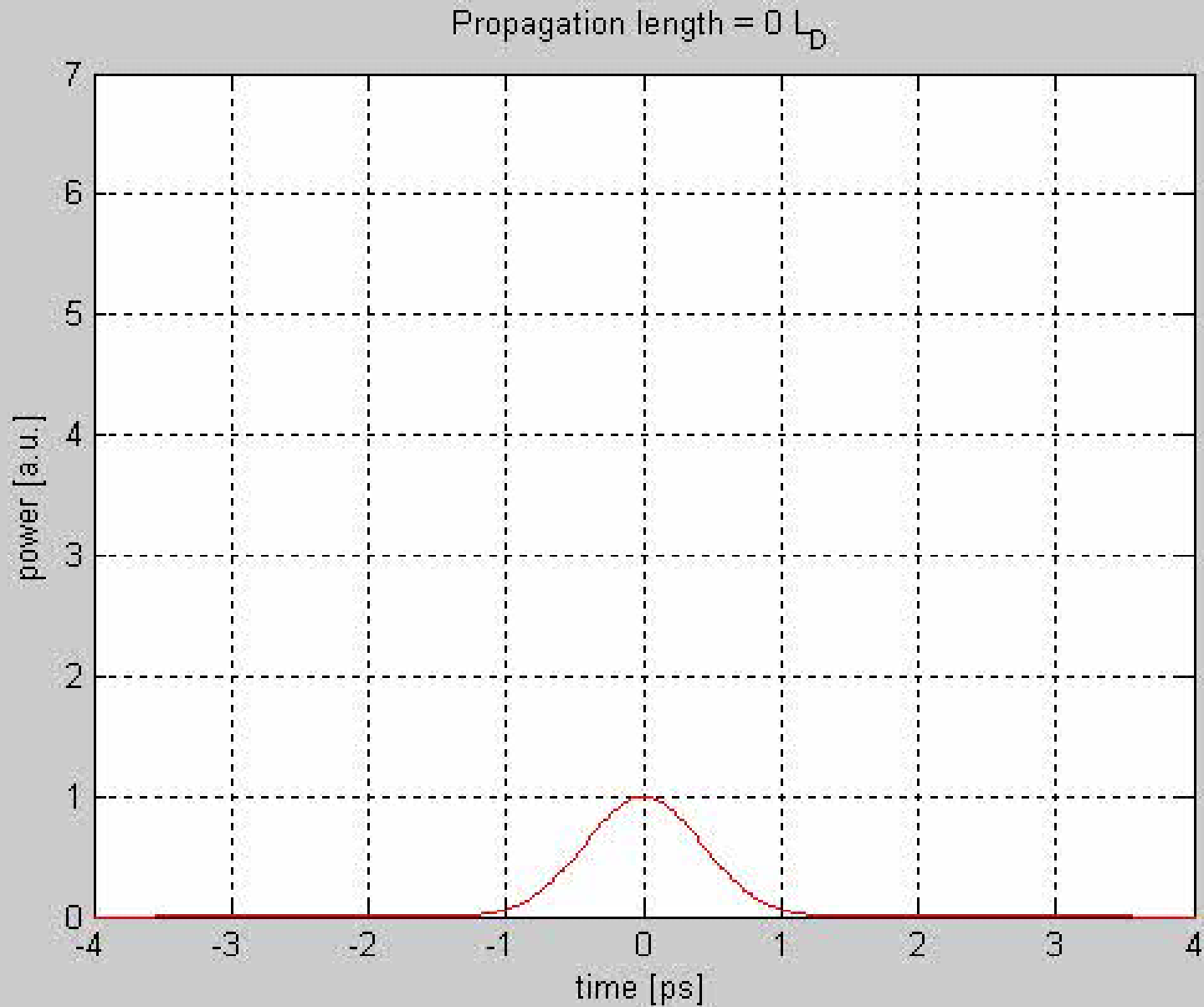
Evolution of a super-Gaussian pulse to soliton
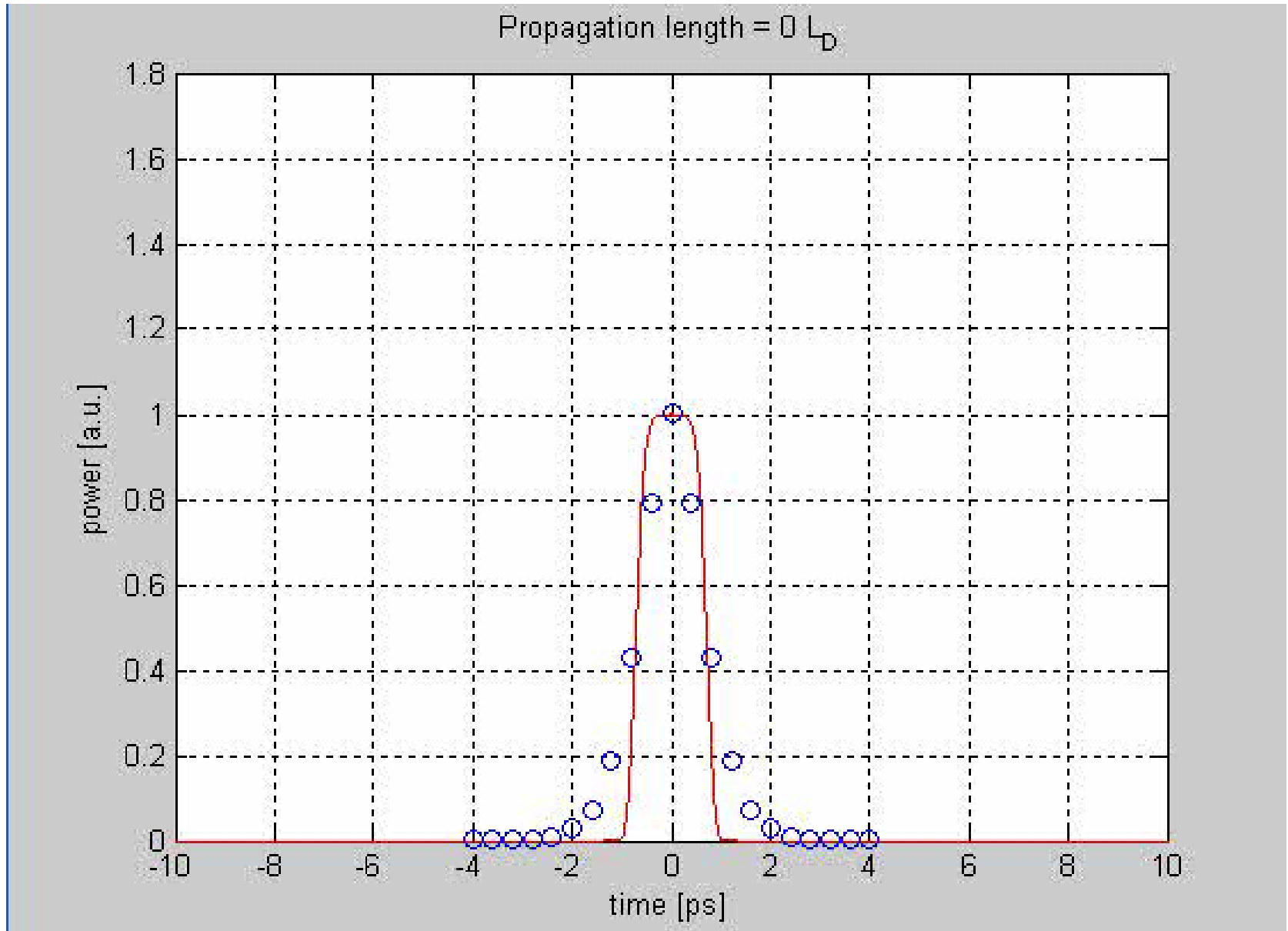
Rogue wave

Find more information from New York times:
http://www.nytimes.com/2006/07/11/science/11wave.html
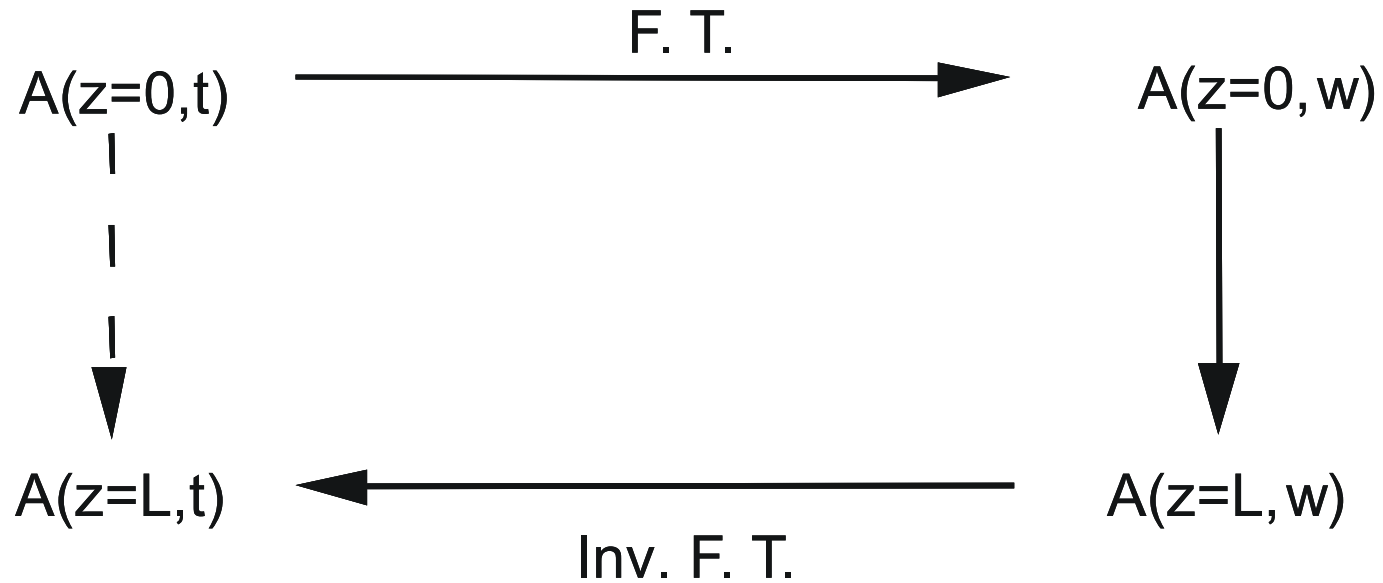
48

One more Rogue wave

Standard Solution of PDEs

Figure 8.9: Fourier Transform method for the solution of linear time invariant PDEs.

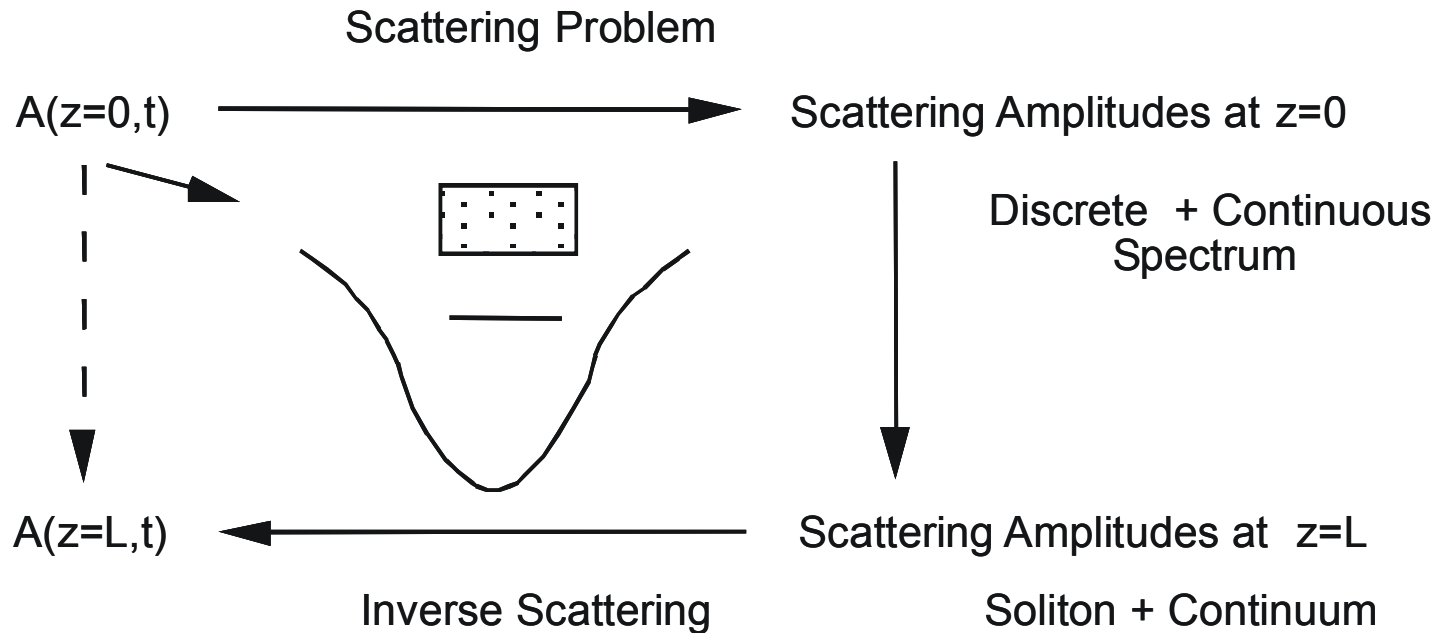# 3.3.4 Inverse Scattering Theory

Figure 8.10: Schematic representation for the inverse scattering theory for the solution of integrable nonlinear partial differential equations

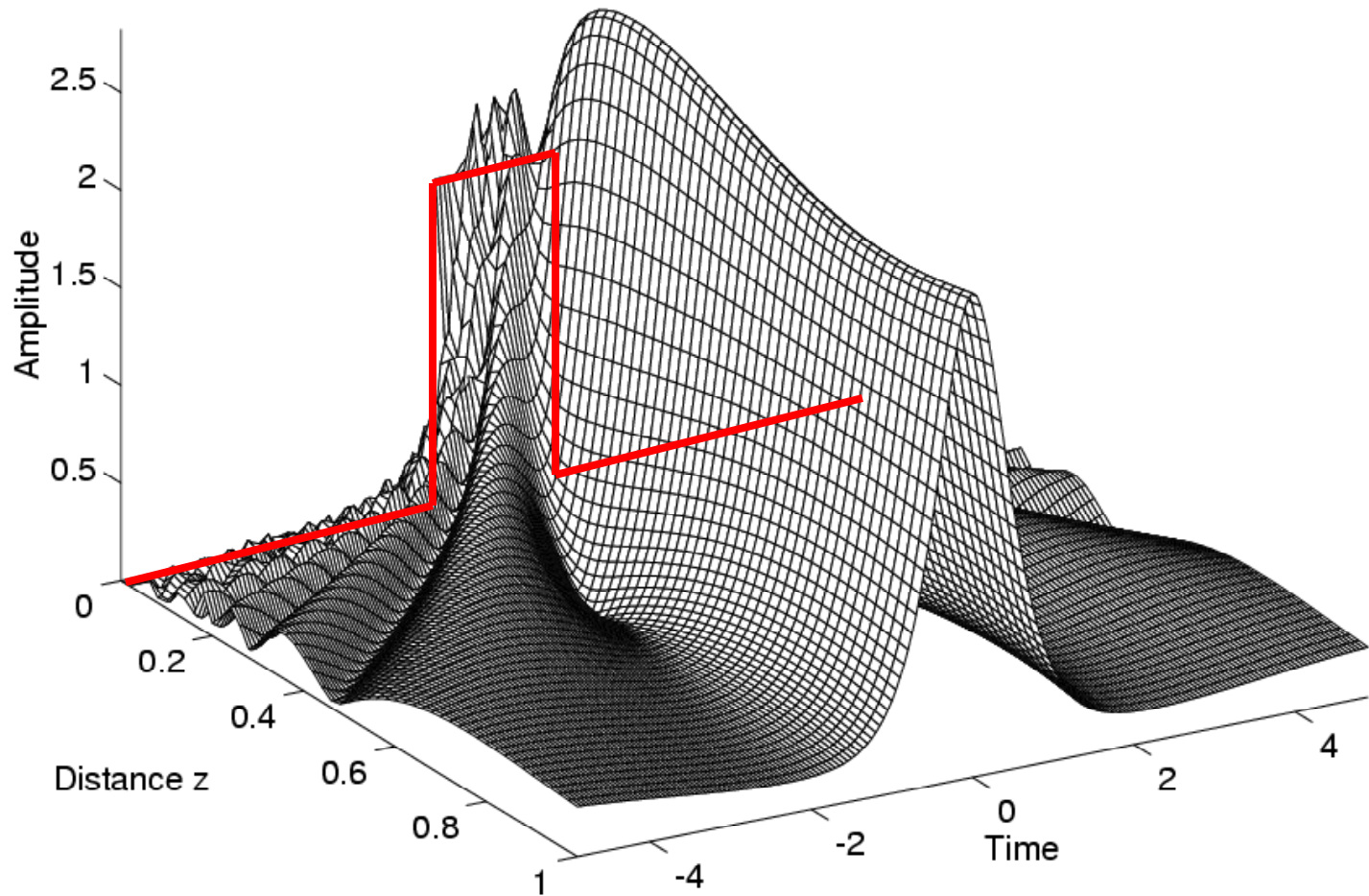# Rectangular Shaped Initial Pulse and Continuum Generation

Figure 8.11: Solution of the NSE for a rectangular shaped initial pulse